Study of Condensed Matter by Neutron Scattering and Complementary Methods

Polymorphism and Initial Structure Modelling of a New Mesogen 9OSBch

M. Kosyl[a,b], W. Zając[c], M.D. Ossowska-Chruściel[a,*] and J. Chruściel[a]

[a]Siedlce University of Natural Sciences and Humanities, Institute of Chemistry, 3-go Maja 54, 08-110 Siedlce, Poland

[b]Joint Institute for Nuclear Research, Laboratory of Neutron Physics
F. Joliot-Curie 6, 141 Dubna, Russian Federation

[c]The Henryk Niewodniczański Institute of Nuclear Physics, Polish Academy of Sciences
E. Radzikowskiego 152, 31-342 Kraków, Poland

We report the properties of a novel mesogen with high temperature cholesteric mesophase, which belongs to an unexplored as yet series of cholesteric esters. This compound is cholesteryl 4-(4-nonyloxybenzoylthio) benzoate ($C_9H_{19}OC_6H_4COSC_6H_4COOch$, where ch = cholesteryl), hereafter named 9OSBch. The chemical structure and purity of 9OSBch was established by ^{1}H NMR, ^{13}C NMR and FT-IR spectroscopy, and its mesomorphism was characterised by differential scanning calorimetry, polarizing optical microscopy, and transmitted light intensity. Differential scanning calorimetry measurements showed that substance is stable up to 270 °C and partially decomposes above this temperature. Observation under polarizing optical microscope revealed oily streak texture of cholesteric phase (Ch). The chemical structure of an isolated molecule was optimized by the density functional theory method. Energetically most favourable configuration is that of hockey stick geometry. At the same time this is the conformation best suited for the formation of highly ordered condensed phases.

DOI: 10.12693/APhysPolA.124.959

PACS: 61.30.Eb, 64.70.M–

1. Introduction

Cholesterol is a well-known natural compound, found e.g. in mammalian cell membranes, with chiral carbon atoms in its molecular structure. Cholesterol is a precursor of numerous biochemical substances as well as of novel chemical forms. Many cholesterol derivatives exhibit cholesteric mesophases, since the presence of the cholesteryl fragment in the molecular structure is one of the requirements towards the formation of mesophase.

The first cholesterol derivative known to exhibit a mesophase was cholesterol benzoate. It was in 1888, when Friedrich Reinitzer observed the melting point of this compound. He noticed the appearance of a muddy liquid instead of expected clear one [1].

Mesogens with cholesterol part still inspire scientist to look for new liquid crystal structures [2, 3]. The studies of these substances intensified during the last 20 years. For example, cholesteric copolysiloxanes with high temperature nematic phase were used as stationary phase in gas chromatography [4]. In medicine copolymer with cholesterol can be used in anticancer drugs and genetic therapy [5]. Highly desired are materials with high thermal stability of the cholesteric phase [6]. Unique properties of cholesteric liquid crystals motivated researchers to construct organic dye lasers. Wide spectral range, from ultraviolet wavelengths, through the visible range, to infrared wavelengths and completely selective reflection of circularly polarized light causes that this laser can be one of the most versatile coherent light sources [7]. Apart from that, esters of cholesterol and higher fat acids are useful components of compound mixtures [8, 9].

Besides extensive research carried out worldwide, the relationship between chemical structure and polymorphism is still far from complete understanding. With this in mind as well as in order to study properties of new compounds, we synthesized a novel thioester homologous series incorporating the cholesteryl fragment and named it nOSBch. The sulphur atom increases thermal stability of the mesogens and broadens the range of liquid crystal phase [10, 11].

In this paper we present the properties of only one homolog, 9OSBch. Detailed description of the synthesis of the whole new series will be presented soon.

2. Experimental

2.1. Materials and methods

2.1.1. Materials

9OSBch (Fig. 1) was synthesized from 4-(4′-nonyloxybenzoylthio)benzoyl chloride and cholesterol. 4-(4′-nonyloxybenzoylthio)benzoyl chloride was obtained by us, while cholesterol was purchased from Aldrich Chemical Company.

2.1.2. Characterization of methods

The structure of 9OSBch was confirmed by elemental analysis EA, IR, ^{1}H NMR, ^{13}C NMR and MS spectroscopic methods. IR spectra were recorded on a FTIR Nicolet Magna 760 spectrometer in the range of 4000–400 cm^{-1} using 64 co-added scans at the resolution of 1 cm^{-1}. The NMR spectra were obtained with V RI N

*corresponding author; e-mail: dch@uph.edu.pl

Unity Plus spectrometer operating at 500 MHz ($CDCl_3$, TMS as internal standard). MS spectra were obtained by MS TOF ES+. The chemical purity was checked by thin layer chromatography TLC and further confirmed by elemental analysis using a Perkin–Elmer 2400 spectrometer. Transition temperatures were established by polarized optical microscopy (POM), transmitted light intensity (TLI) using microscope with Bur–Brown OPT101 photodiode, and differential scanning calorimeter (DSC). Heating and cooling rates for all POM, TLI, and DSC measurements were the same ($\pm 5.0\,^{\circ}C\ min^{-1}$). The temperature was controlled with a Linkam controller with an accuracy of $\pm 0.1\,^{\circ}C$, coupled with Linkam programmable heating stage THMSE 600. A detailed description of our TLI measuring set-up can be found in [13]. DSC measurements were performed using a DSC 822^e Mettler Toledo Star System differential scanning calorimeter.

A Fourier transform infrared (FT-IR) spectrum was recorded for the novel 9OSBch samples in the solid state. The equilibrium geometries, harmonic vibrational frequencies and infrared intensities were computed using the density functional theory (DFT) and the Gaussian 09 package [14], at the Academic Computer Centre CYFRONET AGH, Kraków.

3. Results and discussion

3.1. Spectroscopic data

The chemical structure of 9OSBch is shown in Fig. 1.

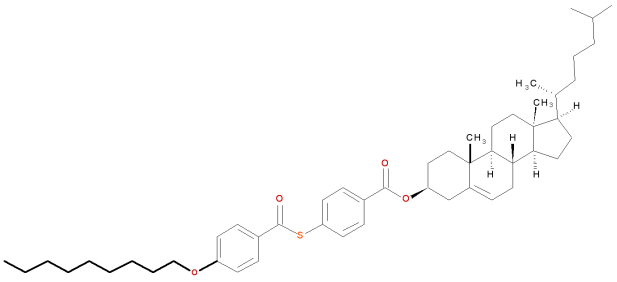

Fig. 1. Chemical structure of 9OSBch.

The NMR data of 9OSBch are as follows: abbreviation: s = singlet, d = doublet, t = triplet, m = multiplet.

^{1}H NMR δ (ppm): alifatic: 0, 69 (s, 3H, $-CH_3$); 0.87 (m, 8H, $-CH_2$); 0.91 (m, 4H, $-CH_2$); 1.07 (m, 13H, –CH, $-CH_2$, $-CH_3$); 1.29 (m, 14H, $-CH_2$); 1.51 (m, 9H, $-CH_3$); 1.79 (m, 4H, $-CH_2$); 1.92 (m, 1H, –CH); 2.07 (m, 3H, $-CH_2$, –CH); 2.47 (d, 2H, $-CH_2$), 4, 03 (t, 2H, $-OCH_2$); 4.88 (m, 1H, O–CH); 5.43 (s, 1H, CH=CH); aromatic: 6.95 (d, 2H, CH); 7.53 (d, 2H, CH); 7.98 (d, 2H, CH); 8.09 (d, 2H, CH).

^{13}C NMR δ (ppm): 187.37 (COO); 165.39 (COS)·aromatic: 163.84, 139.57, 134.71, 133.36, 131.43, 130.02, 129.78, 128.85, 122.87, 114.44, aliphatic: 74.85, 68.41, 56.69, 56.13, 50.04, 42.32, 39.74, 39.51, 38.18, 37.01, 36.65, 36.18, 35.79, 31.93, 31.85, 31.87, 30.91, 29.05–29.34, 28.23, 28.00, 27.86, 25.95, 24.29, 23.82, 22.81, 22.55–22.65, 21.05, 19.37, 18.71, 14.09, 11.86.

Elemental data: experimental: C — 77.98%, H — 9.52%; calculated: C — 78.02%, H — 9.49%.

IR data:

IR (cm^{-1}): ν C–H_{Ar} — 3058.16; ν C–H_{Alkyl} — 2929.35, 2851.64; ν C=O_{COO} — 1721.98, 1705.93; ν C=O_{COS} — 1673.08, 1597.92; ν C=C_{Ar} — 1597.92; ν C–O — 1272.10; ν C–S — 1165.86; δ C–H_{Ar} — 900.23.

3.2. Thermal analysis

Phase transition enthalpies and transition temperatures were determined by DSC (heating rate 5°/min) and the latter confirmed with the TLI method, see Fig. 2.

The sample of 9OSBch (S_1, $m_{S1} = 13.69$ mg) was subjected to a full cycle of heating to 315 °C and cooling to −20 °C (rate 5°/min). The compound was found to decompose at the melting point. During cooling we did not notice any transition.

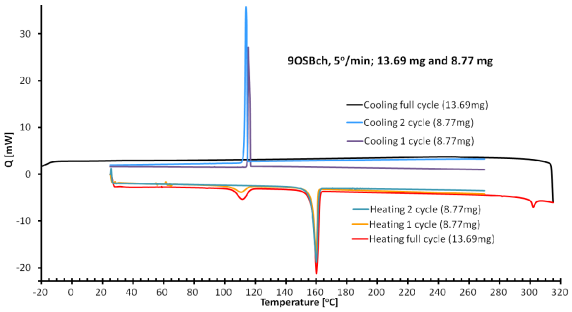

Fig. 2. The DSC curves for third cycles of 9OSBch scans: full cycle for sample S_1 (13.69 mg) — heating 25°–315 °C and cooling from 315° to −20 °C; the first cycle for sample S_2 (8.77 mg) — heating 25°–270 °C and cooling from 270° to −20 °C; the second cycle for the same sample S_2 — heating from −20° to 270 °C and cooling from 270° to 25 °C.

Phase transition temperatures and corresponding enthalpy and entropy changes, obtained on the full cycle are presented in Table I.

TABLE I

The temperature, enthalpy and entropy for full-cycle phase transitions (sample S_1). Sample S_1 (13.69 mg), heating 25°–315 °C; 5°/min.

Transitions	T [°C]	ΔH [J/g]	ΔS [J/(g K)]
Cr2–Cr1	111.34	15.44	0.04016
ACr1–N*	159.26	55.46	0.12826
N*–I	301.50	3.88	0.00675

9OSBch exhibits an enantiotropic cholesteric phase. Transitions are visible during heating: to cholesteric phase at 159.26 °C and at 301.5 °C to isotropic phase, yet after reaching 301.5 °C the compound undergoes decomposition.

The stability of the cholesteric phase is one of the most important parameters influencing the practical use of mesogens. We performed subsequent cycles of heating

and cooling for new samples with the aim to establish the range of stability of the cholesteric phase. One sample of 9OSBch was heated to 290 °C, second one to 280 °C and the last one to 270 °C. We confirmed that cholesteric phase is stable if sample is heated to 270 °C. Table II presents the temperature of phase transitions and corresponding values of enthalpy and entropy for the sample S_2 (8.77 mg), received during heating to the temperature of 270 °C and cooling down from this temperature.

During cooling, the cholesteric phase becomes supercooled by about 42 deg. The low temperature phase transition in 9OSBch visible during heating is the one between two crystalline phases. For an "as-made" crystalline sample, heated for the first time, the transition appears at *ca.* 111 °C, however during subsequent heating cycles it becomes shifted to a considerably lower temperature, i.e. 15–16 °C. The transition Cr1–Cr2 is absent out if sample is heated from room temperature (cycle 3, Table II).

TABLE II

The temperature, enthalpy and entropy phases transitions for sample $S_2 = 8.77$ mg for four measurements. Cycles were performed one after another. The sample was heated to 270 °C and cooled to −20 °C in cycle 1, 3, 4 and to +20 in cycle 2. T [°C], ΔH [J g^{-1}], ΔS [J g^{-1} K^{-1}].

Cycle		Cr2–Cr1			Cr1–Ch			Ch–Cr1		
		T	ΔH	ΔS	T	ΔH	ΔS	T	ΔH	ΔS
1	heating	110.63	11.31	0.03985	159.06	53.28	0.12323			
	cooling							116.31	43.08	0.11065
2	heating	15.46	5.03	0.01743	158.88	53.00	0.12268			
	cooling							115.70	42.64	0.10966
3	heating				158.88	52.39	0.12127			
	cooling							118.18	43.80	0.11193
4	heating	16.04	5.73	0.01981	158.80	52.52	0.12159			
	cooling							116.59	42.96	0.11023
average over $1 \div 4$					158.90	52.80	0.12221	116.70	43.12	0.11061

The temperature values, enthalpies and entropies for phase transitions Cr1–Ch and Ch–Cr1 are similar in all four cycles investigated. The largest deviation from average ΔS observed during four measurements was at the of level 1.06% for transition Cr1–Ch. It can be assumed with high probability that cholesteric phase in 9OSBch is stable up to 270 °C during heating. It spans over *ca.* 111° during heating and *ca.* 153° during cooling.

Phase transition temperatures observed by POM match well those derived from the corresponding DSC thermograms. Different textures of crystalline phases observed using POM method indicate different crystalline forms during heating and cooling. Cholesteric phase of 9OSBch exhibits typical oily-streak textures during heating and cooling cycles, as it is shown in Fig. 3.

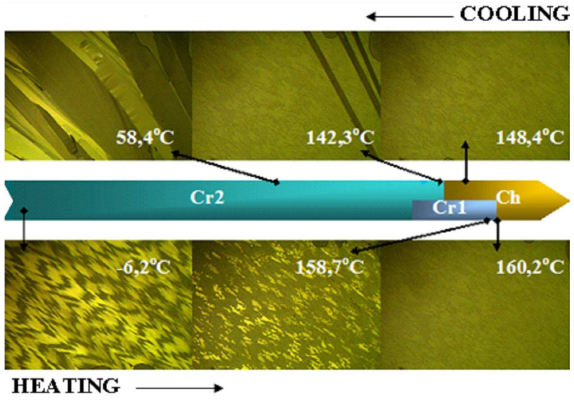

Fig. 3. Textures obtained for 9OSBch during heating and cooling.

3.3. Molecular modelling

For an isolated molecule of 9OSBch functional theory (DFT) calculations were performed using the B3LYP functional with semiempirical dispersion corrections (GD3BJ and PFD), as employed in the Gaussian 09 Rev. D.01 package [14]. The including of dispersion interactions in a relatively large, multi-atomic organic system is necessary. The basis sets used were 6-311G++G(d,p) for atoms in rigid core, and 6-311G otherwise. A uniform approach to all atoms at the high level of theory would be unnecessary, resource-consuming, and would lead to serious convergence problems.

In this paper we report on calculations carried out for an isolated molecule in vacuum, at 0 K, while spectroscopic experiments were performed on solid samples with closely-packed molecules. This leads to typical discrep-

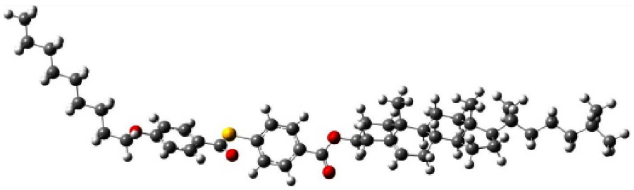

Fig. 4. Equilibrium "hockey-stick" geometry of the 9OSBch molecule obtained from DFT calculations.

ancies between calculated and observed vibrational wave numbers, resulting from the coupling effects of intra- and intermolecular interactions. Intermolecular interactions in an ordered phase are both long-range and local, over distances shorter than the size of the molecule. As an obvious consequence, the impact of the intermolecular interactions is likely to affect the spatial structure of neighbouring molecules, as proved during DFT calculations for a bi-molecular system (work still underway). Several possible conformations were obtained, however usually incapable of forming ordered, closely packed structures. The most plausible and of lowest energy chemical structure of 9OSBch is shown in Fig. 4.

Correctness of the simulated structure was confirmed by IR spectra, obtained from Nicolet Magna 760 spectrometer, a minimum of 64 co-added scans at a resolution of 1 cm^{-1} and theoretical calculation. Figure 5 presents the experimental and theoretical infrared spectra.

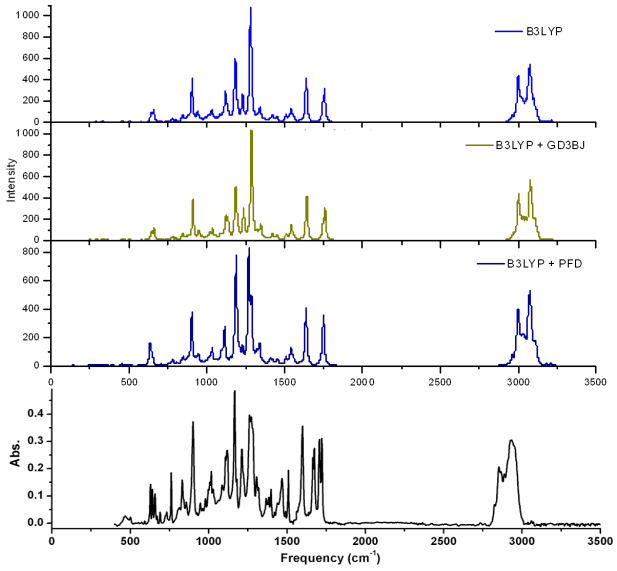

Fig. 5. Comparison of theoretical and experimental of 9OSBch spectra.

The simulated infrared spectra were calculated without semi-empirical dispersion corrections and with two such corrections, GD3BJ and PFD.

Easily noticeable are the differences in the band intensities. For example, the C–O band theoretical spectrum is more intense than the corresponding one in the experimental spectrum. Another possible reason for mismatch of band intensities is the shape and half-width of the individual, often partly overlapping bands, arbitrarily taken to be Lorentzian with FWHM = 12 cm^{-1}.

The experimental wave numbers are tabulated in Table III together with the calculated wave numbers for 9OSBch.

TABLE III

Comparison of the experimental FT-IR wave numbers (cm^{-1}) and theoretical harmonic wave numbers (cm^{-1}) of 9OSBch for main characteristic groups calculated at 0 K, as described in text.

Characteristic group	Experimental FT-IR [cm^{-1}]	Theoretical FT-IR [cm^{-1}]
νC–H_{Ar}	3058.16	3057.98
νC–H_{Alkil}	2929.35	2991.86
νC=$O_{(COO)}$	1721.98; 1705.93	1750.22; 1742.37
νC=$O_{(COS)}$	1673.08	1638.17
νC=C_{Ar}	1597.92	1598.43
νC–C_{Ar}	1506.37	1508.79
ν r–O–CH_2–	1272.10	1229.51
νC–S	1165.86	1187.59
AC–$O_{(COO)}$	1116.78	1114.37
δC–H_{Ar}	900.23	902.98

Intensity of CH group in theoretical spectrum is lower than in the experimental spectrum, however the differences in spectral positions are very small. Small differences between intensities and positions are observed for group C=O in COO and in COS groups.

4. Conclusions

The new compound 9OSBch has a high-temperature cholesteric mesophase. The cholesteric phase exists within a broad temperature range and is stable up to 270 °C. The temperature range of stability of cholesteric phase was confirmed by repeated heating the sample to 270 °C and subsequent cooling. During repeated heating/cooling cycles, almost identical phase transition temperatures were obtained, as well as the values of enthalpy and entropy.

The most probable structure of 9OSBch was determined using DFT method with several types of exchange-correlation functionals. The hockey stick conformation of the 9OABch molecule appears most probable, at the same time capable of forming highly-ordered condensed phase structures. Computed spectra were compared with the FT-IR recorded in the crystalline state. Experimental spectra are very rich in bands.

The best reproduction of the experimental spectra was obtained using B3LYP functional with semi-empirical PFD dispersion corrections.

References

[1] F. Reinitzer, *Monatsh. Chem.* **9**, 421 (1888).

[2] J.S. Hu, *Europ. Polym. J.* **46**, 535 (2010).

[3] J.S. Hu, C. Liu, X. Zhang, Q.-B. Meng, *Europ. Polym. J.* **45**, 3292 (2009).

[4] C.-H. Lin, C.-S. Hsu, *Polymer Bull.* **45**, 53 (2000).

[5] Y.-X. Zhou, V.A. Briand, N. Sharma, S.-K. Ahn, R.M. Kasi, *Materials* **2**, 636 (2009).

[6] N. Tamaoki, G. Kruk, H. Matsuda, *J. Mater. Chem.* **9**, 2381 (1999).

[7] G. Chilaya, A. Chanishvili, G. Petriashvili, R. Barberi, M.P. de Santo, M. Matranga, *Mater. Sci. Appl.* **2**, 116 (2011).

[8] P. Das, S. Basu, R.K. Sinha, U. Das, *Chem. Phys. Lett.* **410**, 417 (2005).

[9] M.I. Serbina, N.L. Liesetski, I.A. Gvozdovskyy, A.V. Kowalchuk, G.S. Chilaya, *Function. Mater.* **17**, 4 (2010).

[10] M.D. Ossowska-Chruściel, Z. Karczmarzyk, J. Chruściel, *Mol. Cryst. Liq. Cryst.* **382**, 37 (2002).

[11] M.D. Ossowska-Chruściel, A. Rudzki, J. Chruściel, *J. Term. Anal. Calorim.* **96**, 835 (2009).

[12] S. Wróbel, Z. Burakowski, J. Chruściel, J. Czerwiec, M. Marzec, M.D. Ossowska-Chruściel, B. Wantusiak, *Phase Transit.* **85**, 379 (2012).

[13] M.D. Ossowska-Chruściel, S. Zalewski, A. Rudzki, A. Filiks, J. Chruściel, *Phase Transit.* **79**, 679 (2006).

[14] Gaussian 09, Revision D.01, M.J. Frisch, G.W. Trucks, H.B. Schlegel, G.W. Trucks, H.B. Schlegel, G.E. Scuseria, M.A. Robb, J.R. Cheeseman, G. Scalmani, V. Barone, B. Mennucci, G.A. Petersson, H. Nakatsuji, M. Caricato, X. Li, H.P. Hratchian, A.F. Izmaylov, J. Bloino, G. Zheng, J.L. Sonnenberg, M. Hada, M.Ehara, K. Toyota, R. Fukuda, J. Hasegawa, M. Ishida, T. Nakajima, Y. Honda, O. Kitao, H. Nakai, T. Vreven, J.A. Montgomery, Jr., J.E. Peralta, F. Ogliaro, M. Bearpark, J.J. Heyd, E. Brothers, K.N. Kudin, V.N. Staroverov, T. Keith, R. Kobayashi, J. Normand, K. Raghavachari, A. Rendell, J.C. Burant, S.S. Iyengar, J. Tomasi, M. Cossi, N. Rega, J.M. Millam, M. Klene, J.E. Knox, J.B. Cross, V. Bakken, C. Adamo, J. Jaramillo, R. Gomperts, R.E. Stratmann, O. Yazyev, A.J. Austin, R. Cammi, C. Pomelli, J.W. Ochterski, R.L. Martin, K. Morokuma, V.G. Zakrzewski, G.A. Voth, P. Salvador, J.J. Dannenberg, S. Dapprich, A.D. Daniels, O. Farkas, J.B. Foresman, J.V. Ortiz, J. Cioslowski, D.J. Fox, Gaussian, Inc., Wallingford CT, 2013.